Tetrahedron Vol. 44, No. 2, pp. 405 to 416, 1988
Printed in Great Britain

0040-4020/88 $3.00+.00
Pergamon Journals Ltd.

STERICALLY CROWDED CYCLOHEXANES - 8[1]. SYNTHESIS, CRYSTAL STRUCTURE, CONFORMATION AND DYNAMICS OF PENTASPIRO[2.0.2.0.2.0.2.0.2.1]HEXADECANE, PENTASPIRO[3.0.2.0.3.0.2.0.3.1]-NONADECANE AND PENTASPIRO[3.0.3.0.3.0.3.0.3.1]HENEICOSANE

Lutz Fitjer*[a], Ulrich Klages[a], Detlef Wehle[a], Manfred Giersig[a], Norbert Schormann[a,b], William Clegg*[b], David S. Stephenson[c] and Gerhard Binsch*[c]

Institut für Organische Chemie der Universität Göttingen[a], Tammannstr. 2, D-3400 Göttingen, Germany,

Institut für Anorganische Chemie der Universität Göttingen[b], Tammannstr. 4, D-3400 Göttingen, Germany, and

Institut für Organische Chemie der Universität München[c], Karlstr. 23, D-8000 München, Germany

(*Received in Germany* 25 *September* 1987)

ABSTRACT

The synthesis, crystal structure (**7,8**), conformation and dynamics of pentaspiro[2.0.2.0.2.0.2.0.2.1]hexadecane **6**, pentaspiro[3.0.2.0.3.0.2.0.3.1]nonadecane **7** and pentaspiro[3.0.3.0.3.0.3.0.3.1]heneicosane **8** are described. Chair conformations have been found in the solid state (**7,8**) and in solution (**6,7,8**). The activation parameters of the chair-to-chair interconversion have been determined from bandshape analyses of exchange broadened ^{1}H-NMR (**6,7**) and ^{13}C-NMR spectra (**8**), respectively. The results were as follows: **6**: $\Delta H^{\ddagger}$ = 48.9 ± 0.8 kJ/mol, $\Delta S^{\ddagger}$ = -20.7 ± 2.8 J/mol·grd, $\Delta G^{\ddagger}_{298}$ = 55.0 ± 0.1 kJ/mol; **7**: $\Delta H^{\ddagger}$ = 51.2 ± 0.7 kJ/mol, $\Delta S^{\ddagger}$ = -12.0 ± 2.4 J/mol·grd, $\Delta G^{\ddagger}_{298}$ = 54.8 ± 0.1 kJ/mol; **8**: $\Delta H^{\ddagger}$ = 74.2 ± 0.6 kJ/mol, $\Delta S^{\ddagger}$ = -21.9 ± 1.5 J/mol·grd, $\Delta G^{\ddagger}_{298}$ = 80.7 ± 0.2 kJ/mol. On the basis of these values the barrier of inversion of the still unknown hexaspirane **5** is predicted to exceed 160 kJ/mol.

1. INTRODUCTION

We reported on the synthesis, conformation and dynamics of the sterically crowded hexaspiranes **1**[2,3], **2**[3], **3**[1] and **4**[1]. Of these, **1** ($\Delta G^{\ddagger}_{298}$ = 89.4 kJ/mol)[3] and **2** ($\Delta G^{\ddagger}_{298}$ = 92.0 kJ/mol)[3] exhibit nearly identical barriers of inversion, but in **3** ($\Delta G^{\ddagger}_{333}$ = 110.0 kJ/mol)[1] and **4** ($\Delta G^{\ddagger}_{423}$ = 136.0 kJ/mol)[1], a dramatic increase in the barriers of inversion is observed. Obviously, this increase is due to a corresponding decrease in the number of alternations. This led to the assumption[1] that the still unknown hexaspirane **5**, which shows no alternations at all, could exhibit the highest barrier of inversion of all cyclohexanes known so far.

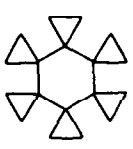

1

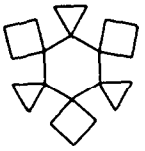

2

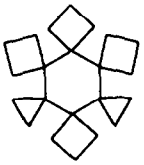

3

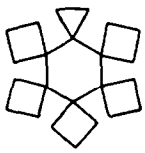

4

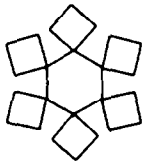

5

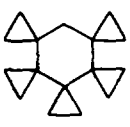

6

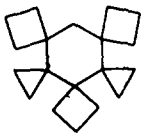

7

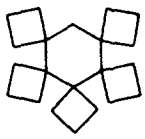

8

*) New address: Department of Inorganic Chemistry, The University, Newcastle upon Tyne, NE1 7RU, U.K.

In order to predict the barrier of inversion of the still unknown hexaspirane **5** more precisely than before, we herein report on a comparative study of the structure, conformation and dynamics of the hexaspiranes **1-4** and the pentaspiranes **6-8**. Of these , **7** is related to both **2** and **3**, and **8** to both **4** and **5**. The pentaspirane **6** was included to answer the question, whether the nearly identical barriers of inversion of **1** and **2** would correspond to nearly identical barriers of inversion of **6** and **7**. In this case the pentaspiranes **7** and **8** were thought to be reliable models for the hexaspiranes **2-4**.

2. SYNTHESES

The pentaspiranes **6** and **7** were obtained from the corresponding ketones **9**[2] and **10**[4] after a modification of the Wolff-Kishner reduction developed by Barton[5]. **8** was produced from trione cis-**11**[6] by the same *method*[7].

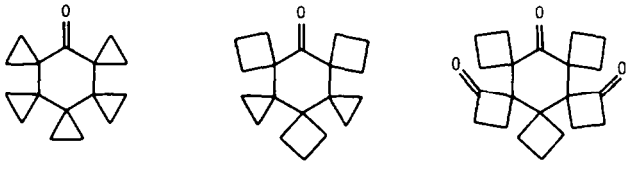

9 **10** **11**

3. CONFORMATION AND DYNAMICS

For the determination of the conformation and dynamics of the pentaspiranes **6**, **7** and **8**, the temperature dependence of the corresponding ^{1}H- (**6**,**7**) and ^{13}C-NMR spectra (**8**) was studied. Within the slow exchange limit, the ^{1}H-NMR spectra of **6** [200 MHz, CD_2Cl_2/CD_3OD (4:1), $CHDCl_2$ int.[8], -80°C; Fig. 1] and **7** [80 MHz, CD_2Cl_2, $CHDCl_2$ int.[8], -70°C; Fig. 2], and the ^{13}C-NMR spectrum of **8** [20 MHz, hexachlorobutadiene, cyclosilane-d_{18} int.[8], +25.7°C; Fig. 3] clearly indicated that in each case the expected chair conformation (C_s-symmetry) was present. In particular, the non-equivalence of the cyclohexane protons in **6** and **7**, and the non-equivalence of the axial and equatorial carbon atoms in **8** was clearly recognized.

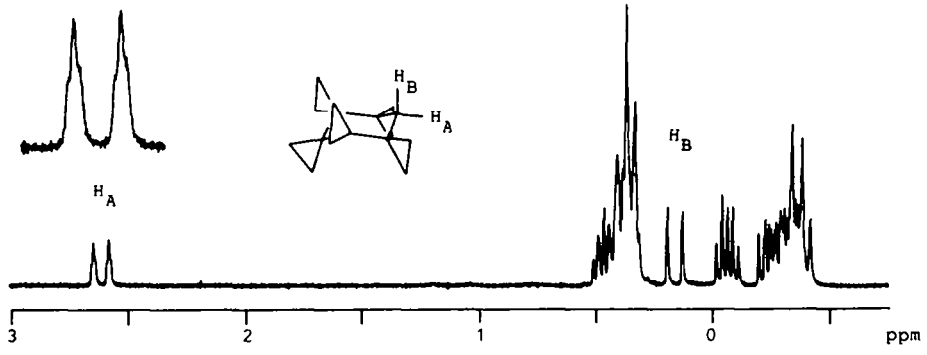

Fig.1. ^{1}H-NMR spectrum [200 MHz, CD_2Cl_2, $CHDCl_2$ int.[8], -80°C] of **6**.

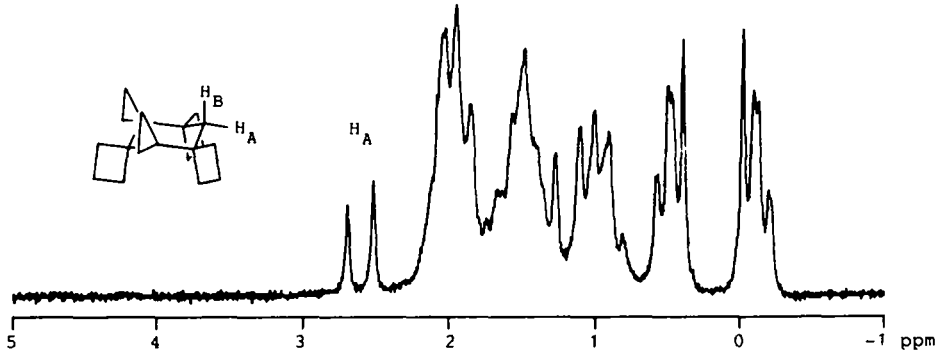

Fig.2. ^{1}H-NMR spectrum [80 MHz, CD_2Cl_2, $CHDCl_2$ int.[8], -70°C) of **7**.

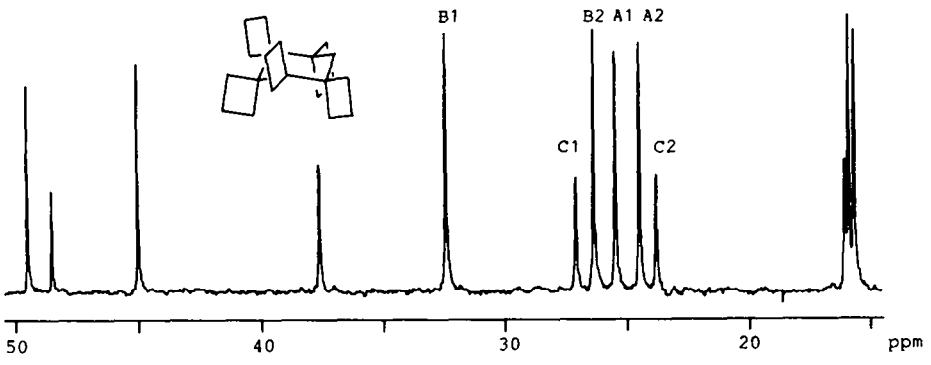

Fig.3. ^{13}C-NMR spectrum [20 MHz, hexachlorobutadiene, cyclosilane-d_{18} int.[8], +25.7°C] of **8**.

In the high resolution ^{1}H-NMR spectrum of **6** (Fig. 1), the protons of the cyclohexane ring form the fully resolved AB-part of an ABC_2-system and therefore - with the exception of δ_C - all static parameters (δ_A = 2.62 ppm, δ_B = 0.16 ppm, J_{AB} = -12.90 Hz, J_{AC} = 1.63 Hz, J_{BC} = 0.00 Hz) could be determined directly. δ_C (= 0.36 ppm) was finally obtained by a ^{1}H- ^{1}H-correlated COSY-experiment[9]. The static parameters were thought to be independent of temperature and field strength and used in a bandshape analysis of the A-part of the ABC_2-system of exchange broadened low resolution 80 MHz ^{1}H-NMR spectra throughout. The spectra were taken at -83.0°C and six further temperatures and the bandshapes and corresponding rate constants calculated using the computer program DNMR 5[10] (Fig. 4). A weighted least squares adjustment of the rate data to the Eyring equation, shown graphically in Fig. 7, then yielded the activation parameters and their standard deviations as $\Delta H^{\ddagger}$ = 48.9 ± 0.8 kJ/mol and $\Delta S^{\ddagger}$ = -20.7 ± 2.8 J/mol·grd. The free energy of activation was then calculated from the equation $\Delta G^{\ddagger} = \Delta H^{\ddagger} - T\Delta S^{\ddagger}$ to give $\Delta G^{\ddagger}_{298}$ = 55.0 ± 0.1 kJ/mol.

By contrast with **6**, the static parameters of the AB-system observed for the cyclohexane protons of **7** were inaccessible because the B-part was overlapped by the protons of the cyclobutane rings (Fig.2). We therefore approximated the ABCD-system to be expected for the protons of the cyclopropane rings by an AA'BB'-system apparently present and used the corresponding static parameters (δH_a = -0.04 ppm, δH_e = 0.56 ppm, $^2J_{ee} = {}^2J_{aa}$ = -0.95 Hz, $^3J_{cis}$ = 8.73 Hz, $^3J_{trans}$ = 5.83 Hz) which were thought to be independent of temperature, in the bandshape analysis of the high temperature spectra throughout. Spectra were taken at -28.1°C and six further temperatures and analyzed by DNMR 5[10]. Experimental and computed bandshapes are shown in Fig. 5, a weighted least squares adjustment of the corresponding rate data in Fig. 7. The activation parameters of the chair-to-chair interconversion resulted as $\Delta H^{\ddagger}$ = 51.2 ± 0.7 kJ/mol and $\Delta S^{\ddagger}$ = -12.0 ± 2.4 J/mol·grd, and the corresponding free energy of activation was calculated as above to give $\Delta G^{\ddagger}_{298}$ = 54.8 ± 0.1kJ/mol.

For the evaluation of the activation parameters of the chair-to-chair interconversion of **8** the three pairs of resonance lines at δ = 24.57 and 25.55 (A1/A2), 26.44 and 32.49 (B1/B2), and 23.90 and 27.18 (C1/C2), representing the axial and equatorial carbon atoms of the three different types of cyclobutane rings (Fig. 3), were used. The analysis of the three non-coupling AB-systems was achieved by a modified DNMR 5-program and, as the frequency differences were not identical ($\Delta\nu_{A1/A2}$ = 19.6 Hz, $\Delta\nu_{B1/B2}$ = 121.0 Hz, $\Delta\nu_{C1/C2}$ = 65.6 Hz at +25.7°C), three different coalescence temperatures were observed. The temperature dependence of the frequency differences was determined by nine measurements ranging from +25.7 to +67.5°C, and a subsequent least squares adjustment to the temperature using the program ACTPAR[11]. Linear relationships resulted in each case [$\Delta\nu_{A1/A2}$ = -(0.037 ± 0.010)·T + (30.79 ± 0.33), $\Delta\nu_{B1/B2}$ = -(0.040 ± 0.011)·T + (132.98 ± 0.36), $\Delta\nu_{C1/C2}$ = -(0.590 ± 0.012)·T + (83.24 ± 0.39)] and especially $\Delta\nu_{C1/C2}$ proved highly temperature dependent. No such dependence was found for the T_2 relaxation times and hence for the bandshape analyses only the temperature dependence of the frequency differences was taken into account. The bandshapes of ten spectra taken within the temperature range from +83.7 to +185.0°C were analyzed by the modified DNMR 5-program (Fig. 6), and from a least squares adjustment of the corresponding rate data to the Eyring equation (Fig. 7) the following activation parameters for the chair-to-chair interconversion of **8** resulted: $\Delta H^{\ddagger}$ = 74.2 ± 0.6 kJ/mol, $\Delta S^{\ddagger}$ = -21.9 ± 1.5 J/mol·grd and $\Delta G^{\ddagger}_{298}$ = 80.7 ± 0.2 kJ/mol.

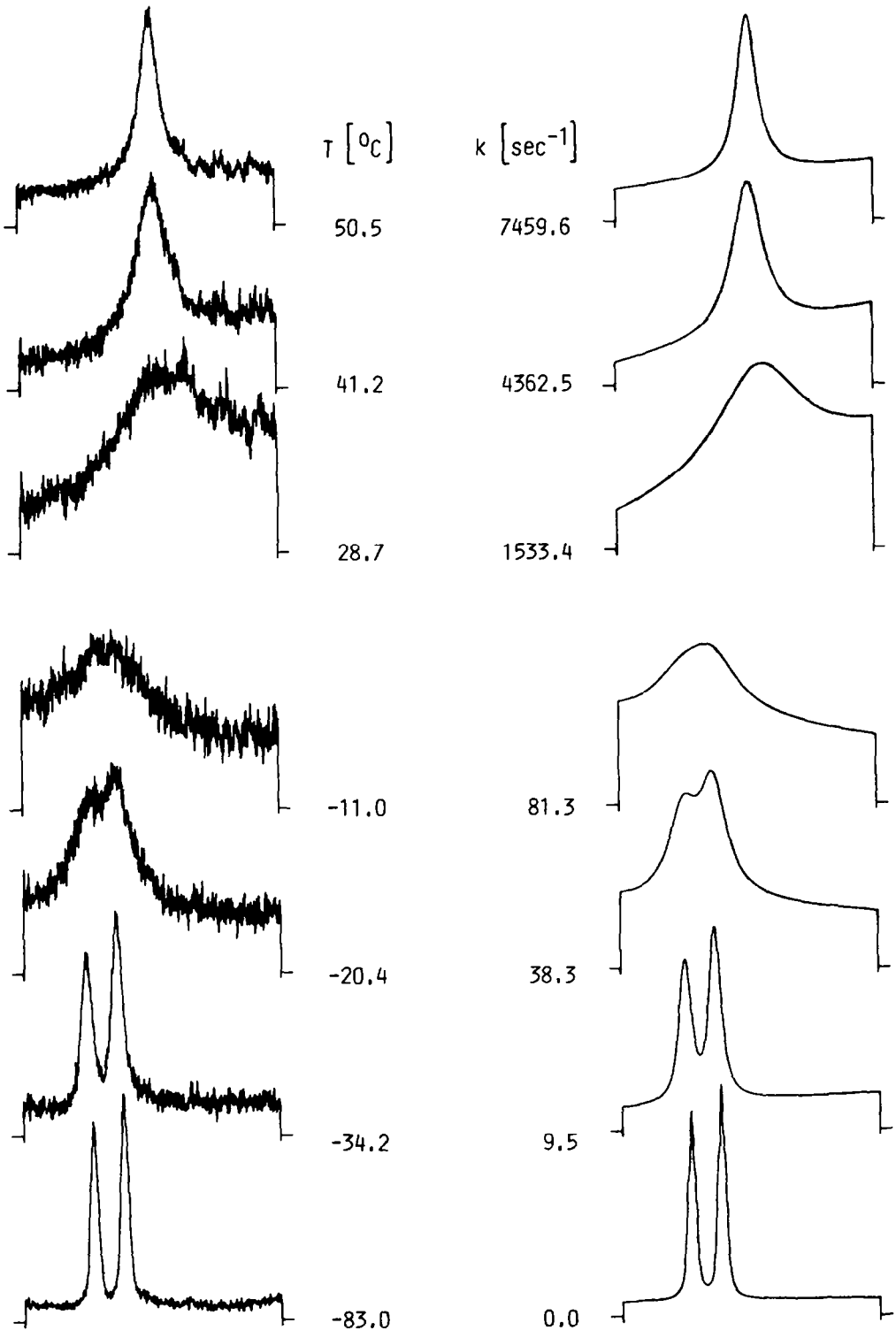

Fig. 4. Experimental and computed bandshapes of the A-part of the ABC_2-system of **6** at different temperatures and corresponding rate constants derived therefrom.

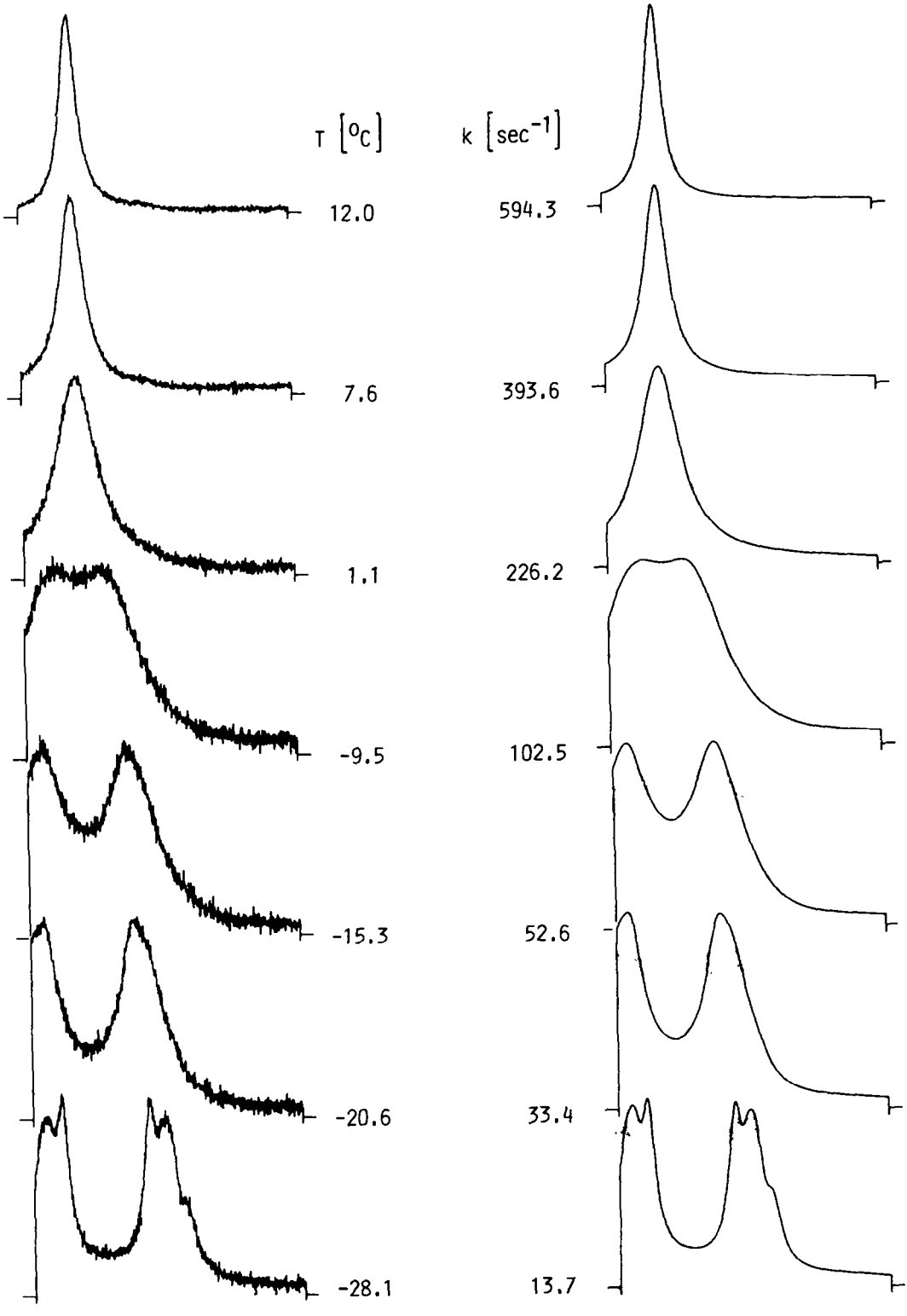

Fig.5. Experimental and computed bandshapes of the cyclopropane part of the ^{1}H-NMR spectrum of 7 at different temperatures and corresponding rate constants derived therefrom.

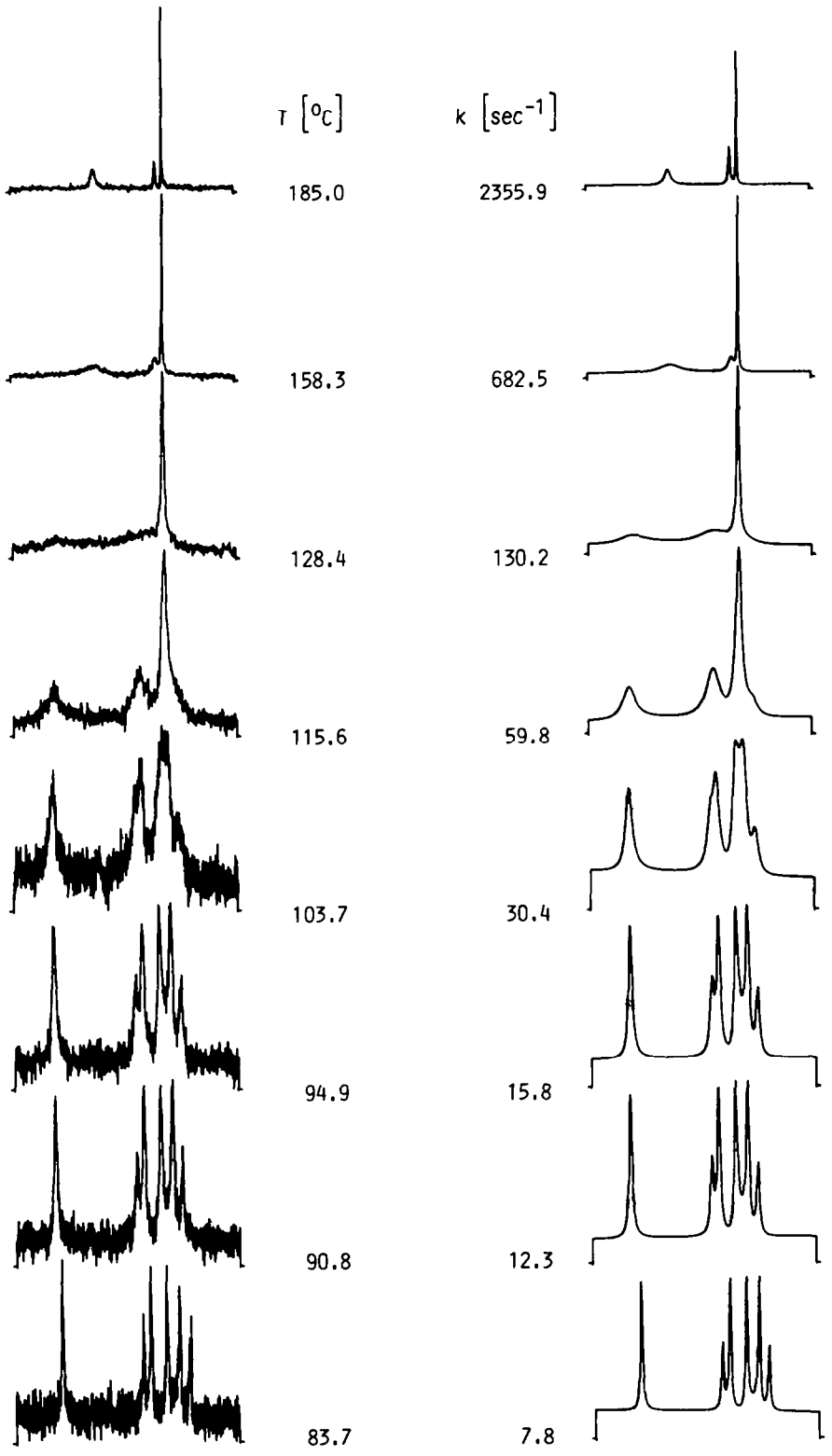

Fig.6. Experimental and computed bandshapes of the non coupling AB-systems of the ^{13}C-NMR spectrum of 8 at different temperatures and corresponding rate constants derived therefrom; measurements at 148.9°C (k = 477.5/sec) and 171.5°C (k = 1262.3/sec) are not shown here but are included in the least squares adjustment of the rate data to the Eyring equation (Fig.7).

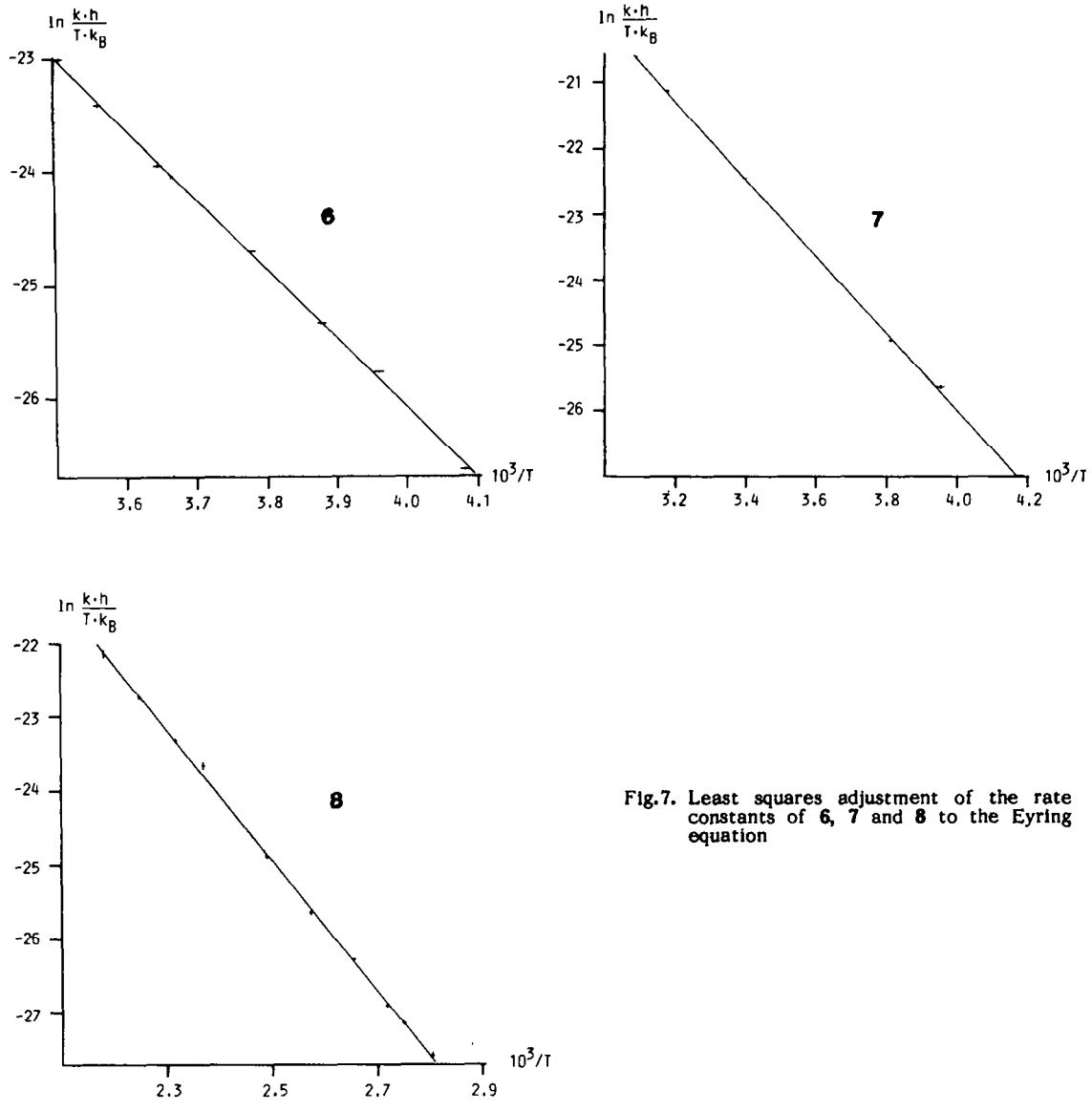

Fig.7. Least squares adjustment of the rate constants of **6**, **7** and **8** to the Eyring equation

4. CRYSTAL STRUCTURES[12]

In a future reparametrization of empirical force fields, especially of the terms describing nonbonding interactions[13], the availability of structural parameters of sterically crowded molecules will be essential. We therefore determined the crystal structure of both **7** and **8**. In the solid state, **7** and **8** adopt a chair conformation with bond lengths (Tables 1,4), bond angles (Tables 2,5) and torsion angles (Tables 3,6) similar to those of their fully cycloalkylated counterparts **3**[1] and **4**[1]. In both cases, the central ring is slightly flattened [$\sum(\omega)$= 316.1° (**7**) and 320.3° (**8**)] and distinct differences in the bond lengths within the cyclobutane rings have been observed. Those to the spiro atoms (average of the opening angles: 87.4°) are somewhat elongated (average: 1.56 Å), and those to the peripheral carbon atoms are somewhat shortened (average: 1.53 Å). All cyclobutane rings in **7** and the two cyclobutane rings located at C(4) and C(19) of **8** are clearly puckered (torsion angles: 11-18°) while the remaining three cyclobutane rings in **8** are nearly planar (torsion angles 1-6°). As in **3**[1] and **4**[1], the non-bonded distances of carbon atoms in 1,2-e,e and 1,2-e,a position are rather short (average: 3.1 Å).

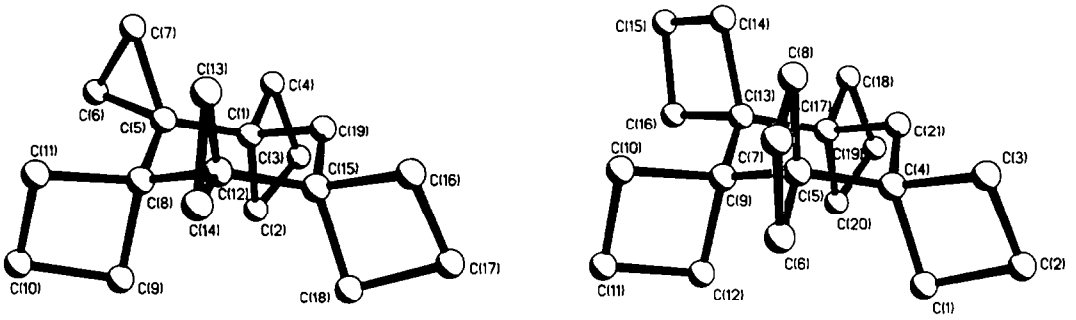

Fig.8. Perspective view of the carbon skeletons of **7** (left) and **8** (right) with the crystallographic atom numbering

C(1)-C(2)	1.573(3)	C(5)-C(6)	1.506(3)	C(8)-C(12)	1.534(3)	C(13)-C(14)	1.501(3)
C(1)-C(4)	1.553(3)	C(5)-C(7)	1.504(3)	C(9)-C(10)	1.529(4)	C(15)-C(16)	1.557(3)
C(1)-C(5)	1.521(3)	C(5)-C(8)	1.530(3)	C(10)-C(11)	1.518(4)	C(15)-C(18)	1.559(3)
C(1)-C(19)	1.526(3)	C(6)-C(7)	1.497(3)	C(12)-C(13)	1.507(3)	C(15)-C(19)	1.529(3)
C(2)-C(3)	1.526(4)	C(8)-C(9)	1.562(3)	C(12)-C(14)	1.500(3)	C(16)-C(17)	1.529(3)
C(3)-C(4)	1.533(3)	C(8)-C(11)	1.561(3)	C(12)-C(15)	1.525(3)	C(17)-C(18)	1.525(3)

Table 1. Bond lengths (Å) for **7** with estimated standard deviations in parentheses

C(2)-C(1)-C(4)	87.2(1)	C(5)-C(6)-C(7)	60.1(1)	C(13)-C(12)-C(15)	117.6(1)
C(2)-C(1)-C(5)	116.8(1)	C(5)-C(7)-C(6)	60.3(1)	C(14)-C(12)-C(15)	118.0(2)
C(4)-C(1)-C(5)	119.0(2)	C(5)-C(8)-C(9)	113.7(2)	C(12)-C(13)-C(14)	59.8(1)
C(2)-C(1)-C(19)	114.9(2)	C(5)-C(8)-C(11)	114.0(2)	C(12)-C(14)-C(13)	60.3(1)
C(4)-C(1)-C(19)	109.0(2)	C(9)-C(8)-C(11)	87.5(1)	C(12)-C(15)-C(16)	118.5(1)
C(5)-C(1)-C(19)	108.7(1)	C(5)-C(8)-C(12)	109.4(1)	C(12)-C(15)-C(18)	117.8(1)
C(1)-C(2)-C(3)	89.1(2)	C(9)-C(8)-C(12)	114.6(2)	C(16)-C(15)-C(18)	86.8(1)
C(2)-C(3)-C(4)	89.6(2)	C(11)-C(8)-C(12)	116.4(2)	C(12)-C(15)-C(19)	109.7(2)
C(1)-C(4)-C(3)	89.6(2)	C(8)-C(9)-C(10)	89.9(2)	C(16)-C(15)-C(19)	108.4(1)
C(1)-C(5)-C(6)	117.4(2)	C(9)-C(10)-C(11)	90.3(2)	C(18)-C(15)-C(19)	113.9(1)
C(1)-C(5)-C(7)	116.1(2)	C(8)-C(11)-C(10)	90.3(2)	C(15)-C(16)-C(17)	89.3(1)
C(6)-C(5)-C(7)	59.7(1)	C(8)-C(12)-C(13)	118.0(2)	C(16)-C(17)-C(18)	89.0(2)
C(1)-C(5)-C(8)	114.4(2)	C(8)-C(12)-C(14)	118.9(2)	C(15)-C(18)-C(17)	89.3(1)
C(6)-C(5)-C(8)	120.2(2)	C(13)-C(12)-C(14)	59.9(1)	C(1)-C(19)-C(15)	116.8(1)
C(7)-C(5)-C(8)	118.3(2)	C(8)-C(12)-C(15)	114.1(1)		

Table 2. Bond angles (°) for **7** with estimated standard deviations in parentheses

C(1)-C(5)-C(8)-C(12)	55.8(2)	C(8)-C(9)-C(10)-C(11)	-10.8(2)	C(4)-C(1)-C(5)-C(7)	-35.6(2)
C(5)-C(8)-C(12)-C(15)	-54.2(2)	C(9)-C(10)-C(11)-C(8)	10.8(2)	C(6)-C(5)-C(8)-C(9)	74.3(2)
C(8)-C(12)-C(15)-C(19)	51.1(2)	C(9)-C(8)-C(11)-C(10)	-10.6(2)	C(6)-C(5)-C(8)-C(11)	-23.9(2)
C(12)-C(15)-C(19)-C(1)	-50.4(2)	C(11)-C(8)-C(9)-C(10)	10.5(2)	C(7)-C(5)-C(8)-C(11)	45.6(2)
C(5)-C(1)-C(19)-C(15)	51.2(2)	C(15)-C(16)-C(17)-C(18)	-17.9(2)	C(9)-C(8)-C(12)-C(14)	-71.8(2)
C(19)-C(1)-C(5)-C(8)	-53.4(2)	C(16)-C(17)-C(18)-C(15)	17.9(2)	C(11)-C(8)-C(12)-C(13)	-41.0(2)
C(1)-C(2)-C(3)-C(4)	-15.9(2)	C(16)-C(15)-C(18)-C(17)	-17.6(2)	C(11)-C(8)-C(12)-C(14)	28.2(2)
C(2)-C(3)-C(4)-C(1)	16.1(2)	C(18)-C(15)-C(16)-C(17)	17.5(2)	C(13)-C(12)-C(15)-C(16)	31.9(2)
C(2)-C(1)-C(4)-C(3)	-15.6(2)	C(2)-C(1)-C(5)-C(6)	-70.5(2)	C(14)-C(12)-C(15)-C(16)	-36.8(2)
C(4)-C(1)-C(2)-C(3)	15.7(2)	C(4)-C(1)-C(5)-C(6)	32.1(2)	C(14)-C(12)-C(15)-C(18)	65.6(2)

Table 3. Selected torsion angles (°) for **7** with estimated standard deviations in parentheses

C(1)-C(2)	1.521(5)	C(5)-C(8)	1.569(4)	C(10)-C(11)	1.525(4)	C(15)-C(16)	1.527(5)
C(1)-C(4)	1.568(4)	C(5)-C(9)	1.540(4)	C(11)-C(12)	1.535(6)	C(17)-C(18)	1.561(6)
C(2)-C(3)	1.531(6)	C(6)-C(7)	1.539(5)	C(13)-C(14)	1.567(4)	C(17)-C(20)	1.570(4)
C(3)-C(4)	1.563(5)	C(7)-C(8)	1.529(6)	C(13)-C(16)	1.566(4)	C(17)-C(21)	1.519(5)
C(4)-C(5)	1.529(5)	C(9)-C(10)	1.576(5)	C(13)-C(17)	1.533(5)	C(18)-C(19)	1.522(6)
C(4)-C(21)	1.531(5)	C(9)-C(12)	1.570(4)	C(14)-C(15)	1.529(5)	C(19)-C(20)	1.521(7)
C(5)-C(6)	1.571(5)	C(9)-C(13)	1.544(5)				

Table 4. Bond lengths (Å) for **8** with estimated standard deviations in parentheses

C(2)-C(1)-C(4)	89.9(2)	C(6)-C(7)-C(8)	90.8(3)	C(14)-C(13)-C(17)	111.6(3)
C(1)-C(2)-C(3)	90.2(3)	C(5)-C(8)-C(7)	90.7(3)	C(16)-C(13)-C(17)	113.3(3)
C(2)-C(3)-C(4)	89.7(3)	C(5)-C(9)-C(10)	113.4(3)	C(13)-C(14)-C(15)	90.6(2)
C(1)-C(4)-C(3)	87.3(2)	C(5)-C(9)-C(12)	114.0(2)	C(14)-C(15)-C(16)	90.4(3)
C(1)-C(4)-C(5)	118.4(3)	C(10)-C(9)-C(12)	88.1(2)	C(13)-C(16)-C(15)	90.8(2)
C(3)-C(4)-C(5)	117.5(3)	C(5)-C(9)-C(13)	112.8(2)	C(13)-C(17)-C(18)	117.7(3)
C(1)-C(4)-C(21)	113.5(3)	C(10)-C(9)-C(13)	113.1(2)	C(13)-C(17)-C(20)	118.5(3)
C(3)-C(4)-C(21)	109.2(3)	C(12)-C(9)-C(13)	113.2(2)	C(18)-C(17)-C(20)	86.8(3)
C(5)-C(4)-C(21)	109.3(3)	C(9)-C(10)-C(11)	90.4(2)	C(13)-C(17)-C(21)	109.3(3)
C(4)-C(5)-C(6)	112.7(3)	C(10)-C(11)-C(12)	91.3(3)	C(18)-C(17)-C(21)	109.4(3)
C(4)-C(5)-C(8)	112.3(3)	C(9)-C(12)-C(11)	90.2(2)	C(20)-C(17)-C(21)	113.5(3)
C(6)-C(5)-C(8)	88.2(3)	C(9)-C(13)-C(14)	115.0(3)	C(17)-C(18)-C(19)	90.1(3)
C(4)-C(5)-C(9)	112.1(3)	C(9)-C(13)-C(16)	115.6(3)	C(18)-C(19)-C(20)	90.0(3)
C(6)-C(5)-C(9)	114.8(3)	C(14)-C(13)-C(16)	87.6(2)	C(17)-C(20)-C(19)	89.9(3)
C(8)-C(5)-C(9)	114.7(2)	C(9)-C(13)-C(17)	111.8(2)	C(4)-C(21)-C(17)	117.2(3)
C(5)-C(6)-C(7)	90.3(3)				

Table 5. Bond angles (°) for **8** with estimated standard deviations in parentheses

C(4)-C(5)-C(9)-C(13)	-54.1(3)	C(8)-C(5)-C(6)-C(7)	-1.1(3)	C(1)-C(4)-C(5)-C(6)	50.3(4)
C(5)-C(9)-C(13)-C(17)	54.3(3)	C(9)-C(10)-C(11)-C(12)	1.0(3)	C(3)-C(4)-C(5)-C(6)	-52.5(3)
C(9)-C(13)-C(17)-C(21)	-51.7(3)	C(10)-C(11)-C(12)-C(9)	-1.0(3)	C(3)-C(4)-C(5)-C(8)	45.2(4)
C(13)-C(17)-C(21)-C(4)	53.5(3)	C(10)-C(9)-C(12)-C(11)	1.0(3)	C(6)-C(5)-C(9)-C(10)	45.4(3)
C(5)-C(4)-C(21)-C(17)	-53.1(3)	C(12)-C(9)-C(10)-C(11)	-1.0(3)	C(6)-C(5)-C(9)-C(12)	-53.4(4)
C(21)-C(4)-C(5)-C(9)	51.0(3)	C(13)-C(14)-C(15)-C(16)	6.3(3)	C(8)-C(5)-C(9)-C(10)	-54.6(4)
C(1)-C(2)-C(3)-C(4)	-13.0(3)	C(14)-C(15)-C(16)-C(13)	-6.3(3)	C(10)-C(9)-C(13)-C(14)	56.0(3)
C(2)-C(3)-C(4)-C(1)	12.6(3)	C(14)-C(13)-C(16)-C(15)	6.2(3)	C(10)-C(9)-C(13)-C(16)	-43.8(3)
C(2)-C(1)-C(4)-C(3)	-12.7(3)	C(16)-C(13)-C(14)-C(15)	-6.2(3)	C(12)-C(9)-C(13)-C(16)	54.5(4)
C(4)-C(1)-C(2)-C(3)	13.0(3)	C(17)-C(18)-C(19)-C(20)	13.8(3)	C(14)-C(13)-C(17)-C(18)	-46.8(3)
C(5)-C(6)-C(7)-C(8)	1.1(3)	C(18)-C(19)-C(20)-C(17)	-13.7(3)	C(16)-C(13)-C(17)-C(18)	50.1(3)
C(6)-C(7)-C(8)-C(5)	-1.1(3)	C(18)-C(17)-C(20)-C(19)	13.4(3)	C(16)-C(13)-C(17)-C(20)	-52.1(4)
C(6)-C(5)-C(8)-C(7)	1.1(3)	C(20)-C(17)-C(18)-C(19)	-13.4(3)		

Table 6. Selected torsion angles (°) for **8** with estimated standard deviations in parentheses

5. DISCUSSION

As we have pointed out earlier[1,3], the barrier of inversion of the still unknown hexaspirane **5** should be extremely high. Based on the free energies of activation of the chair-to-chair interconversion of the hexaspiranes **2**[3], **3**[1] and **4**[1], and the pentaspiranes **7** and **8**, we feel now able to predict this barrier more precisely than before.

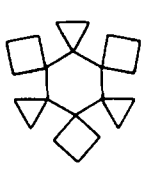

2

$\Delta G^{\ddagger}_{298}$ = 92.0 kJ/mol

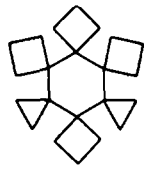

3

$\Delta G^{\ddagger}_{333}$ = 112.1 kJ/mol

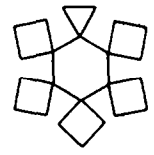

4

$\Delta G^{\ddagger}_{423}$ = 136.0 kJ/mol

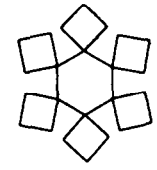

5

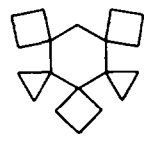

7

$\Delta G^{\ddagger}_{298}$ = 54.8 kJ/mol

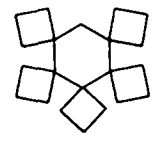

8

$\Delta G^{\ddagger}_{298}$ = 80.7 kJ/mol

As may be calculated from the data given above, identical structural changes correspond to nearly identical percentual changes in the corresponding barrier of inversion. This has been found true for the exchange of one cyclopropane by one cyclobutane ring (**2-3** and **3-4**; $\Delta G^{\ddagger}$ = +22/+21%), for the exchange of two cyclopropane by two cyclobutane rings (**7-8** and **2-4**; $\Delta G^{\ddagger}$ = +47/+48%), and for the incorporation of one new cyclopropane ring (**7-2** and **8-4**; $\Delta G^{\ddagger}$ = +67/+68%). Although we do not have a reasonable explanation of this phenomenological finding, we suppose that the barrier of inversion of the hexaspirane **5** may be estimated not only by use of the increments for the exchange of one (**4-5**; $\Delta G^{\ddagger}$ = +22%) and two cyclopropane rings (**3-5**; $\Delta G^{\ddagger}$ = +48%), but also by use of the increment for the incorporation of one new cyclobutane ring (**8-5**; $\Delta G^{\ddagger}$ = +105%) where only one experimental value (**7-3**; $\Delta G^{\ddagger}$ = +105%) is available. The results of all three calculations fall within the narrow range of 165-166 kJ/mol. We therefore expect that the barrier of inversion of the hexaspirane **5** will exceed 160 kJ/mol, thus making **5** another candidate for conformational isomerism which has already been observed with **3**[1] and **4**[1]. A possible explanation on the basis of nonbonding interactions must await a comparative force-field study on the structure, conformation and dynamics of **2**, **3**, **4**, **5**, **7** and **8**, which is in progress.

6. EXPERIMENTAL

IR spectra were recorded on a Perkin-Elmer 298 spectrophotometer. ^{1}H- and ^{13}C-NMR spectra were measured on a Varian FT 80A or XL200 spectrometer. Mass spectra were obtained with a Varian MAT 731 operated at 70 eV. Analytical gas chromatography was carried out on a Varian 920 instrument employing a thermal conductivity detector and hydrogen as carrier gas. R_f-values are quoted for Machery & Nagel Polygram SIL G/UV$_{254}$ plates. Colourless substances were detected by oxidation with 3.5% alcoholic 12-molybdophosphoric acid (Merck) and subsequent warming. Melting points are not corrected.

Pentaspiro[2.0.2.0.2.0.2.0.2.1]hexadecane 6: 100 mg (4.30 mmol) sodium metal was treated with 10 ml of diethylene glycol under stirring and nitrogen and then 1.00 g (31.0 mmol) anhydrous hydrazine and 90 mg (0.40 mmol) **9**[2] were added. The mixture was heated to 125°c for 16h, and then the temperature was raised to 160°C until tlc analysis [pentane; R_f = 0.02 (**9**) and 0.55 (**6**)] indicated that the reaction was complete (48h). The mixture was cooled, diluted with water (10 ml) and extracted with pentane (3 x 20 ml). The pentane phases were concentrated and the residue (100 mg yellowish oil) chromatographed on silica gel (0.05-0.20 mm) in pentane (column 40 x 2.5 cm) to yield 30 mg (36%) of pure **6** as colourless oil which crystallized on cooling. Recrystallization from acetone yielded colourless crystals which sublimed above 120°C. - IR (CCl_4): 3070, 2995, 2950, 2915, 2860 cm^{-1} (CH). - ^{1}H-NMR (80 MHz, $CDCl_3$, $CHCl_3$ int.[8], +57°C): δ = 0.00-0.20 (s and m, 20H), 1.43 (s, 2H). - ^{13}C-NMR (50.3 MHz, CH_2Cl_2, $CDCl_3$ int.[8], 80°C): δ = 0.24, 0.99, 4.47, 9.35, 9.60, 10.38, 22.03, 25.00 (coincidence of two lines), 43.86. - MS (70 eV): m/e = 186 (50%, M^+-C_2H_4), 129 (100%). Calculated for $C_{14}H_{18}$ (M^+-C_2H_4): 186.1408; Found: 186.1408.

Pentaspiro[3.0.2.0.3.0.2.0.3.1]nonadecane 7: 250 mg (10.9 mmol) sodium metal was treated with 15 ml of diethylene glycol under stirring and nitrogen and then 2.50 g (78.0 mmol) anhydrous hydrazine and 290 mg (1.07 mmol) **10**[4] were added. The mixture was heated to 125°C for 16h, and then the temperature was raised to 170°C until glpc analysis [2.0m x 1/4" all-glass system, 10% OV 101 on chromosorb W AW/DMCS 60/80 mesh, 200°C; rel. retention times: 1.00 (**7**) and 1,44 (**10**)] indicated that the reaction was complete (48h). The mixture was cooled, diluted with water (15 ml) and extracted with pentane (3 x 20 ml). The pentane phases were concentrated and the residue (350 mg yellowish oil) chromatographed on silica gel (0.05-0.20 mm) in pentane [column 40 x 2.5 cm; R_f = 0.03 (**10**) and 0.61 (**7**)] to yield 255 mg (93%) of pure **7** as colourless oil which crystallized on cooling. Recrystallization from acetone/water yielded colourless needles (mp 56°C). - IR (film): 3070-2820 cm^{-1} (CH). - ^{1}H-NMR (80 MHz, CD_2Cl_2, $CHDCl_2$ int.[8], -64°C): δ = 0.45 (AA'BB', 8H), 0.95-2.45 (m, 19H), 2.71 (A-part of an AB-system, J_{AB} = 14.5 Hz, 1H). - ^{13}C-NMR (50.3 MHz, symm. $C_2D_2Cl_4$[8], +140°C): δ = 3.44, 15.77, 16.04, 26.85, 31.54, 28.33, 43.95, 46.04, 47.05. - MS (70 eV): m/e = 228 (2%, M^+-C_2H_4), 172 (100%). - $C_{19}H_{28}$ requires C, 88.98; H, 11.02. Found: C, 88.84; H, 11.18.

Crystal structure analysis of 7: **7** (molecular formula $C_{19}H_{28}$, M = 256.4) was crystallized from acetone as colourless needles, space group $P2_1/n$, $\underline{a}$ = 8.571(1), $\underline{b}$ = 14.949(1), $\underline{c}$ = 12.328(1) Å, $\underline{\beta}$ = 105.21(1)°, $\underline{V}$ = 1524.2 Å^3, $\underline{Z}$ = 4, $\underline{D}_c$ = 1.117 g·cm^{-3}. 2682 reflections[14] with $2\Theta_{max}$ = 50° were measured on a Stoe four-circle diffractometer using graphite-monochromated Mo-Kα radiation; of these, 2237 with $|F|>3\sigma_F$

were used for the structure determination and refinement. The structure was solved by direct methods and refined isotropically to R = 0.173, which dropped to R = 0.127 with inclusion of anisotropic temperature factors. At this stage all H atoms were located by a difference electron density synthesis. The anisotropic refinement of the C atoms with geometrically positioned H atoms and isotropically refined H coordinates finally converged at R = 0.060 (R_w = 0.061). C atom parameters are listed in Table 7[12].

	x	y	z	U*		x	y	z	U*
C(1)	4867(2)	3562(1)	2311(1)	38(1)	C(11)	5102(2)	974(1)	1692(2)	56(1)
C(2)	3552(2)	3997(1)	1315(2)	48(1)	C(12)	7182(2)	2275(1)	1736(1)	35(1)
C(3)	3383(3)	4761(1)	2096(2)	69(1)	C(13)	8508(2)	1789(1)	2573(2)	51(1)
C(4)	4255(3)	4194(2)	3110(2)	62(1)	C(14)	8266(3)	1639(1)	1336(2)	58(1)
C(5)	4762(2)	2556(1)	2462(1)	37(1)	C(15)	7405(2)	3275(1)	1578(1)	34(1)
C(6)	3377(2)	2208(1)	2881(2)	58(1)	C(16)	9150(2)	3640(1)	1728(2)	52(1)
C(7)	5049(2)	2230(1)	3652(2)	55(1)	C(17)	8524(2)	4230(1)	692(2)	58(1)
C(8)	5429(2)	1998(1)	1643(1)	36(1)	C(18)	7020(2)	3641(1)	353(2)	46(1)
C(9)	4308(3)	1987(1)	418(2)	52(1)	C(19)	6609(2)	3805(1)	2349(2)	37(1)
C(10)	3776(4)	1036(2)	602(2)	100(1)					

*Equivalent isotropic U defined as one third of the trace of the orthogonalized U_{ij} tensor

Table 7. Atomic coordinates ($\cdot 10^4$) and equivalent isotropic displacement parameters ($Å^2 \cdot 10^3$) for **7** with estimated standard deviations in parentheses

Crystal structure analysis of 8: **8** (molecular formula $C_{21}H_{32}$, M = 284.5) was crystallized from acetone as colourless needles, space group $P\bar{1}$, a = 8.042(1), b = 9.465(1), c = 11.551(2) Å, α = 79.43(1), β = 75.38(1), γ = 88.34(2)°, V = 836.2 $Å^3$, Z = 2, D_c = 1.13 $g \cdot cm^{-3}$. 2185 reflections[14] with $2\Theta_{max}$ = 45° were measured on a Stoe four-circle diffractometer using graphite-monochromated Mo-K_α radiation; of these, 1403 with $|F| > 3\sigma_F$ were used for the structure determination and refinement. The structure was solved by direct methods and refined isotropically to R = 0.159, which dropped to R = 0.144 with inclusion of anisotropic temperature factors. At this stage all H atoms were located by a difference electron density synthesis. Anisotropic refinement of the C atoms and isotropic refinement of the H atoms finally converged at R = 0.069 (R_w = 0.056). C atom parameters are listed in Table 8[12].

	x	y	z	U*		x	y	z	U*
C(1)	5114(4)	129(4)	2045(3)	57(2)	C(12)	3396(4)	2856(4)	394(3)	50(1)
C(2)	5192(6)	-1257(5)	2935(4)	90(2)	C(13)	1929(4)	3411(3)	2536(3)	42(1)
C(3)	3260(5)	-1185(4)	3502(3)	69(2)	C(14)	144(5)	3522(4)	3452(4)	52(2)
C(4)	3268(4)	402(3)	2819(3)	47(1)	C(15)	199(5)	5158(4)	3064(4)	68(2)
C(5)	1854(4)	826(3)	2157(3)	45(1)	C(16)	1829(5)	5063(3)	2062(3)	60(2)
C(6)	1722(4)	-208(4)	1262(3)	62(2)	C(17)	3355(4)	3024(4)	3199(3)	46(1)
C(7)	-44(5)	-765(4)	2078(4)	80(2)	C(18)	3450(5)	3870(4)	4221(3)	63(2)
C(8)	33(4)	253(4)	2949(3)	57(2)	C(19)	5384(6)	4071(5)	3702(4)	84(2)
C(9)	1940(4)	2437(3)	1598(3)	40(1)	C(20)	5228(4)	3603(4)	2542(3)	63(2)
C(10)	587(4)	2886(3)	827(3)	53(2)	C(21)	3260(4)	1422(4)	3707(3)	51(1)
C(11)	2036(5)	3308(4)	-319(3)	68(2)					

*Equivalent isotropic U defined as one third of the trace of the orthogonalized U_{ij} tensor

Table 8. Atomic coordinates ($\cdot 10^4$) and equivalent isotropic displacement parameters ($Å^2 \cdot 10^3$) for **8** with estimated standard deviations in parentheses

Variable temperature measurements: Spectra were recorded on a Varian FT 80A spectrometer equipped with a variable temperature probe. Precision 5 mm o.d. NMR tubes (No.507 PP, Wilmad Glass Co.) were filled with solutions of 10 mg **6** in 500 µl CD_2Cl_2/CD_3OD (4:1), 10 mg **7** in 450 µl CD_2Cl_2 and 160 mg **8** in 360 µl hexachlorobutadiene/cyclosilane-d_{18} (8:1). In the case of **7** and **8** a temperature sensor consisting of a 1.8 mm-diameter high precision PT 100 resistor (1/5 DIN; accuracy ± 0.05°C from 0°C to +200°C) at the end of a glass rod was introduced, such that the active zone (15 mm length) was positioned 10 mm above the height of the receiver coil but was still immersed in the solution. Immediately before and after taking a spectrum, the sensor was moved precisely to the height of the receiver coil, connected to a dual channel digital temperature-measuring instrument (Model S 1220, Systemteknik, Sweden; resolution 0.01°C) and the temperature measured against molten ice. Spectra for which the temperatures from these two measurements differed by more than 0.3°K were discarded and rerun. To avoid trapping of water the NMR probe of **6** was degassed and sealed under nitrogen. In this case immediately before and after taking a spectrum the temperature of an open dummy probe filled with the same solvent mixture as described

for **6** was measured following the same procedure as described for **7** and **8**. Spectra for which the temperatures from these two measurements differed by more than 0.7°C were discarded and rerun.

Calculations: The calculations of the static and dynamic spectra and the weighted least-squares adjustments of the rate data to the Eyring equation were performed on the Sperry Univac 1100 computer of the Gesellschaft für Wissenschaftliche Datenverarbeitung at Göttingen, employing the computer programs DNMR 5[10], a modified version of DNMR 5 and ACTPAR[11], respectively.

Acknowledgements: Financial support of the Deutsche Forschungsgemeinschaft (project Fi 191/7-2) and the Fonds der Chemischen Industrie is gratefully acknowledged. U.K and D.W. thank the Fonds der Chemischen Industrie for a Chemiefonds fellowship.

REFERENCES AND NOTES

1) Part 7: L.Fitjer, M.Giersig, D.Wehle, M.Dittmer, G.-W.Koltermann, N.Schormann and E.Egert, **Tetrahedron 43** (1987); preceeding paper in this issue.

2) L.Fitjer, **Angew. Chem. Int. Ed. Engl. 12**, 763 (1976); L.Fitjer, **Chem. Ber. 115**, 1047 (1982).

3) L.Fitjer, U.Klages, W.Kühn, D.S.Stephenson, G.Binsch, M.Noltemeyer, E.Egert and G.M.Sheldrick, **Tetrahedron 40**, 4337 (1984).

4) L.Fitjer, W.Kühn, U.Klages, E.Egert, W.Clegg, N.Schormann and G.M.Sheldrick, **Chem. Ber. 117**, 3075 (1984).

5) D.H.R.Barton, D.A.J.Ives and B.R.Thomas, **J. Chem. Soc. (London) 1955**, 2056.

6) L.Fitjer, M.Giersig, W.Clegg, N.Schormann and G.M.Sheldrick, **Tetrahedron Lett. 24**, 5351 (1983).

7) M.Giersig, D.Wehle, L.Fitjer, N.Schormann and W.Clegg, submitted to **Chem. Ber.**

8) For standards other than TMS the following chemical shifts were used: $\delta_H(CHCl_3)$ = 7.27, $\delta_H(CHDCl_2)$ = 5.32, δ_C(symm. $C_2D_2Cl_4$) = 86.45, $\delta_C(CDCl_3)$ = 77.00, δ_C(cyclosilane-d_{18}, $\underline{CH_2}$Si-group) = 2.39 ppm.

9) A.Bax and R.Freeman, **J. Magn. Reson. 44**, 542 (1981).

10) D.S.Stephenson and G.Binsch, **J. Magn. Reson. 32**, 145 (1978); D.S.Stephenson and G.Binsch, **Quantum Chemistry Program Exchange 11**, 365 (1978).

11) G.Binsch and H.Kessler, **Angew. Chem. Int. Ed. Engl. 19**, 411 (1980).

12) All relevant crystallographic data have been deposited with the Cambridge Crystallographic Database via the Fachinformationszentrum Energie, Physik, Mathematik, D-7514 Eggenstein-Leopoldshafen 2 (CSD-52692).

13) A recent computational force field study on the sterically crowded all-cis-1,2,3,4,5,6-hexamethyl cyclohexane using five different force fields gave rather poor results: B.van de Graaf, J.M.A.Baas and H.A.Widya, **Recl. Trav. Chim. Pays-Bas 100**, 59 (1981).

14) W.Clegg, **Acta Crystallogr., Sect. A 37**, 22 (1981).